Libyan Journal of Science & Technology 9:2 (2019) 122–128

Faculty of Science - University of Benghazi

Libyan Journal of Science & Technology

journal home page: www.sc.uob.edu.ly/pages/page/77

Performance assessment of the vortex panel method

Khalid M. Sultan*, Anas M. Elshabli, Mohammed A. Kashbour, Seraj A. Ben.Ateiga

Department of Mechanical Engineering, Faculty of Engineering, University of Benghazi, Benghazi,. Libya.

Highlights

- **The vortex panel method has its strength and weakness points.**
- **The method is computationally cheap and relatively easy to program.**
- **The method is capable of solving the incompressible flow past thin airfoils at small angle of attack.**
- **The method can not capture shock waves even if they are weak.**
- **Friction is completely ignored by the method.**

ARTICLE INFO

Article history:
Received 06 August 2018
Revised 10 December 2018
Accepted 17 December 2018
Available online 15 June 2019

Keywords:
Vortex panel method; Potential flow solutions; Kutta condition; CFX; Matlab.

* Corresponding author:
E-mail address: dr-Khalid-Sultan@hotmail.de
K. M. Sultan

ABSTRACT

The vortex panel method is a very simple and computationally effective method to solve the incompressible and inviscid flow past thin airfoils. This work tries to provide a complete and detailed presentation of the mathematical derivation of this method. It also highlights the points of strength and weakness of this method as compared with more advanced yet expensive computational methods. The results obtained from this work have shown that the method is capable of solving the flow past thin airfoils with good precision for subsonic and laminar flow. For transonic and turbulent flows and as the angle of attack of the flow is increased, the method lacks the precision, especially near the leading and trailing edges.

1. Introduction

Numerical methods are nowadays very essential in the aerospace industry. A Simple method such as the vortex panel method is still used in large companies that produce commercial aircraft, especially in the preliminary design stage. The vortex panel method offers a faster and easier alternative as compared to more time consuming both Navier–Stokes and Euler flow solvers due to the fact that the vortex panel method does not require the process of computational grid generation.

2. Mathematical model

The basic equations of fluid motion are called alternatively as the "conservation laws" because they are basically a representation of the three concepts: conservation of mass, conservation of linear momentum, alternatively called Newton's second law of motion, and conservation of energy. In this section, the first two conservation laws will be reviewed in details whereas the third law will be excluded. The panel method, which is the main subject of this study, is based on mass conservation and linear momentum conservation, and it has nothing to do with energy conservation. That is why the conservation of energy is considered as an "out of the scope" subject.

$$\vec{\nabla}.\vec{V} = 0 \tag{1}$$

$$\rho\left[\frac{\partial \vec{V}}{\partial t} - \vec{V}\times\left(\vec{\nabla}\times\vec{V}\right) + \vec{\nabla}\left(\frac{\vec{V}^2}{2}\right)\right] = \rho\vec{g} - \vec{\nabla}P \tag{2}$$

$$u = \frac{\partial \psi}{\partial y}, \qquad v = -\frac{\partial \psi}{\partial x} \tag{3}$$

$$u = \frac{\partial \phi}{\partial x}; \qquad v = \frac{\partial \phi}{\partial y}; \qquad w = \frac{\partial \phi}{\partial z} \tag{4}$$

In this study, the fluid is assumed to be steady, incompressible, irrotational, inviscid, and two-dimensional. Applying the above - mentioned assumptions, and recalling that the continuity equation can be represented by an equivalent total velocity potential function equation in the case of potential flow, Eqs. 1 and 2 are reduced to the following equations:

$$\phi_T = \phi_{v1} + \phi_{v2} = \phi_1 + \phi_2 = \frac{\Gamma_1}{2\pi}\theta_1 + \frac{\Gamma_2}{2\pi}\theta_2 \tag{5}$$

$$P + \frac{1}{2}\rho V^2 + \rho g(Z - Z_o) = P_o \tag{6}$$

In the case of panel codes, the direct implementation of the wall boundary condition would be to mathematically state that the velocity normal to the surface is zero, see (White, 2003).

$$\vec{V}.\vec{n} = 0 \tag{7}$$

The Kutta condition states that in order to obtain a lift from the airfoil, the fluid flow at the trailing edge must satisfy the following condition:

$$V_{upper}(at\ trailing\ edge) = V_{lower}(at\ trailing\ edge) \tag{8}$$

A computer program written by (Kireny, 2002) was employed in this paper. This program implements the variable vortex panel method explained by (Kuethe and Chow, 2009). Although the original computer program, which was introduced by (Kuethe and Chow, 2009) has been written in FORTRAN, the program of (Kireny, 2002) is written in MATLAB. MATLAB is considered a fourth–generation programing language, which has the advantage

© 2019 University of Benghazi. All rights reserved. ISSN 2663-1407; National Library of Libya, Legal number: 390/2018

of containing many embedded libraries. Those libraries were developed, tested, and tweaked to provide the most exact solution for several mathematical problems without sacrificing the speed of computation. Moreover, MATLAB has a built-in plotter, which enables the user to see and investigate the results after the computation.

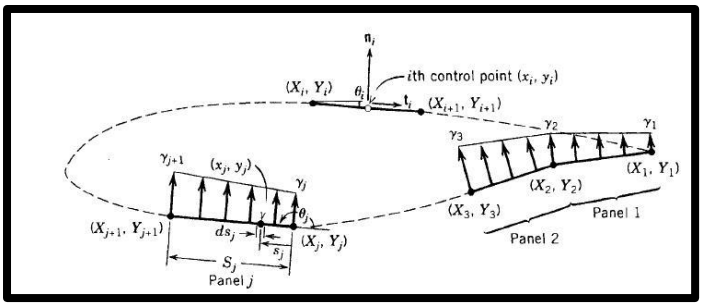

Fig.1. Control Point at Mid Panel (Kuethe and Chow, 2009).

The main idea behind the panel method is in employing the velocity potential instead of the velocity components (u, v) to represent each elementary flow component incorporated in the complex flow at hand. The complex flow at hand in this situation is constructed of a free stream having a velocity of V_∞ at an angle of attack $(\propto)$ and a set of vortex panels (m vortex panels), see Fig. 1. Employing the superposition method to write the equation of the total velocity potential for panel i yields:

$$\emptyset_{(x_i,y_i)} = V_\infty(x_i cos \propto + y_i sin \propto) + \sum_{j=1}^{m} \int_{panel\ j} \frac{-\gamma(s_j)}{2\pi} \tan^{-1}\left[\frac{y_i - y_j}{x_i - x_j}\right] . ds_j \quad (9)$$

It is possible to obtain two equations for the normal and tangential velocity components on panel i as:

$$V_{n_i} = V_\infty(cos\alpha\hat{\imath} + sin\alpha\hat{\jmath}).\vec{n} + \sum_{j=1}^{m} \gamma'_j \int_0^{s_j} f1_n(s_j).ds_j + \gamma'_{j+1} \int_0^{s_j} f2_n(s_j).ds_j \quad (10)$$

$$V_{t_i} = V_\infty(cos\alpha\hat{\imath} + sin\alpha\hat{\jmath}).\vec{t} + \sum_{j=1}^{m} \gamma'_j \int_0^{s_j} f1_t(s_j).ds_j + \gamma'_{j+1} \int_0^{s_j} f2_t(s_j).ds_j \quad (11)$$

Eq. 11 will be dealt with later*. Now concentrating on Eq. 10, the estimation of the two integrals is lengthy and tedious algebraic task. The result is directly given below as:

$$\int_0^{s_j} f1_n(s_j).ds_j = Cn1_{ij} \quad (12-a)$$

$$\int_0^{s_j} f2_n(s_j).ds_j = Cn2_{ij} \quad (12-b)$$

$Cn1_{ij}$ and $Cn2_{ij}$ are coefficients expressed by:

$$Cn1_{ij} = 0.5DF + CG - Cn2_{ij} \quad (13)$$

$$Cn2_{ij} = D + 0.5\frac{QF}{S_j} - \frac{(AC + DE)G}{S_j} \quad (14)$$

The intermediate constants appearing on the right -hand sides of Eqs 13 and 14 and some later expressions are defined as:

$$A = -(x_i - X_j)cos\theta_j - (y_i - Y_j)sin\theta_j$$

$$B = (x_i - X_j)^2 + (y_i - Y_j)^2$$

$$C = sin(\theta_i - \theta_j)$$

$$D = cos(\theta_i - \theta_j)$$

$$E = (x_i - X_j)\, sin\theta_j - (y_i - Y_j)cos\theta_j$$

$$F = \ln\left[1 + \frac{S_j{}^2 + 2AS_j}{B}\right]$$

$$G = \tan^{-1}\left[\frac{ES_j}{B + AS_j}\right]$$

$$P = (x_i - X_j)\sin(\theta_i - 2\theta_j) + (y_i - Y_j)cos(\theta_i - 2\theta_j)$$

$$Q = (x_i - X_j)\cos(\theta_i - 2\theta_j) - (y_i - Y_j)sin(\theta_i - 2\theta_j)$$

Note that these constants are functions of the coordinates of the i^{th} control points, those of the boundary points of the j^{th} vortex panel, and the orientation angles of both i^{th} and j^{th} panels. They can be computed for all possible values of i and j once the panel geometry is specified. Eq. 10 will be employed to write a set of equations for the induced velocity at panel i from all of the remaining panels including the induced velocity from the variable vortex on panel i itself. In addition to this set of equations, the Kutta condition in form of the following equation is added:

$$\gamma'_1 + \gamma'_{m+1} = 0 \quad (15)$$

This will construct a system of (m+1) simultaneous algebraic equations as:

$$\begin{bmatrix} A_{n_{1,1}} & A_{n_{1,2}} & \cdots & A_{n_{1,m}} & A_{n_{1,m+1}} \\ A_{n_{2,1}} & A_{n_{2,2}} & \cdots & A_{n_{2,m}} & A_{n_{2,m+1}} \\ \vdots & \vdots & \cdots & \vdots & \vdots \\ A_{n_{m-1,1}} & A_{n_{m-1,2}} & \cdots & A_{n_{m-1,m}} & A_{n_{m-1,m+1}} \\ A_{n_{m,1}} & A_{n_{m,2}} & \cdots & A_{n_{m,m}} & A_{n_{m,m+1}} \\ 1 & 0 & 0\cdots & 0 & 1 \end{bmatrix} \begin{bmatrix} \gamma'_1 \\ \gamma'_2 \\ \vdots \\ \gamma'_{m-1} \\ \gamma'_m \\ \gamma'_{m+1} \end{bmatrix} = \begin{bmatrix} RHS_1 \\ RHS_2 \\ \vdots \\ RHS_{m-1} \\ RHS_m \\ 0 \end{bmatrix} \quad (16)$$

where:

$$RHS_i = sin(\theta_i - \alpha) \qquad i = 1,2, \ldots\ldots\ldots m+1$$

$A_{n_{ij}}$ is known as the influence coefficient for the normal velocity.

In which, for $\underline{i \neq m+1}$

$$if \quad j = 1 \qquad A_{n_{i1}} = Cn1_{i1}$$

$$if \quad j = 2,3, \ldots\ldots m \qquad A_{n_{ij}} = Cn1_{ij} + Cn2_{ij}$$

$$if \quad j = m+1 \qquad A_{n_{im+1}} = Cn2_{im+1}$$

$$RHS_i = sin(\theta_i - \alpha)$$

And for $\underline{i = m+1}$

$$if \quad j = 1\ and\ j = m+1 \qquad A_{n_{i1}} = A_{n_{im+1}} = 1$$

$$if \quad j = 2,3, \ldots\ldots\ldots\ldots m \qquad A_{n_{ij}} = 0$$

$$RHS_i = 0$$

This system of linear algebraic equations lends itself to solution by the Gauss elimination method to obtain the (m+1) unknowns of γ'_js. Having γ'_js at hand will enable the calculation of the tangential velocity and hence the pressure at the control points. This task will be accomplished by recalling Eq. 11 and substituting for the values of γ'_js in it. The only unknown in Eq. 11 will be the tangential velocities at each panel. Here again, the two integrals on the right-hand side of Eq. 11 will undergo to a lengthy mathematical manipulation and the result is directly given below as:

$$\int_0^{s_j} f1_t(s_j).ds_j = Ct1_{ij} \quad (17-a)$$

$$\int_0^{s_j} f2_t(s_j).ds_j = Ct2_{ij} \quad (17-b)$$

Where:

*The normal velocity component is dealt with firstly because of the boundary condition, which states that this component is equal to zero.

$$Ct1_{ij} = 0.5CF - DG - Ct2_{ij} \quad (18)$$

$$Ct2_{ij} = C + \frac{0.5PF}{S_j} + \frac{(AD - CE)G}{S_j} \quad (19)$$

The constants appearing in Eqs. 18 and 19 are the same constants that appeared when $Cn1_{ij}$ and $Cn2_{ij}$, were calculated. A special case arise when $i = j$, the coefficients have the simplified values:

$$Ct1_{ij} = Ct2_{ij} = \frac{\pi}{2}$$

The local *dimensionless velocity* defined as $V_i = \left[{V_{t_i}}/{V_\infty}\right]$ can be computed as:

$$V_i = \cos(\theta_i - \alpha) + \sum_{j=1}^{m+1} A_{t_{ij}} \cdot \gamma'_j \quad (20)$$

Where $i = 1,2,\dots,m$ and $A_{t_{ij}}$ is known as the influence coefficient for the tangential velocity.

$A_{t_{ij}}$ can be obtained as follows:

$$if \quad j = 1 \qquad A_{t_{i1}} = Ct1_{i1}$$

$$if \quad j = 2,3,\dots\dots\dots m \qquad A_{t_{ij}} = Ct1_{ij} + Ct2_{ij}$$

$$if \quad j = m+1 \qquad A_{t_{i,m+1}} = Ct2_{i,m+1}$$

The γ'_j is already known and the only unknown now is V_i at each control point.

We can determine V_i for each panel by:

$$[V_i] = [\cos(\theta_i - \alpha)] + \left[A_{t_{ij}}\right]\left[\gamma'_j\right] \quad (21)$$

After solving Eq. 21 for each panel, the values of the dimensionless velocity at each control point can be obtained. We can calculate the pressure coefficient at each control point by Bernoulli's law and using dimensionless velocity V_i at each control point, that is:

$$C_{p_i} = 1 - {V_i}^2 \quad (22)$$

3. Results and discussions

3.1 Determination of the Optimum Panel Count

The effect of airfoil thickness on the panel count can be investigated by examination of Figs. 2 to 6. In each figure, six solutions are shown. These solutions are obtained using twenty, forty, eighty, one hundred and twenty, one hundred and sixty, and two hundred panels. As seen in these figures the solutions obtained by using both twenty and forty panels deviate considerably from the other solutions. These deviations occur especially at the regions of high gradients, namely; near the leading and the trailing edges. Another important notice here is that all the remaining obtained solutions are coincident. This means that increasing the panel count above eighty is superfluous and will not lead to any improvement in the accuracy.

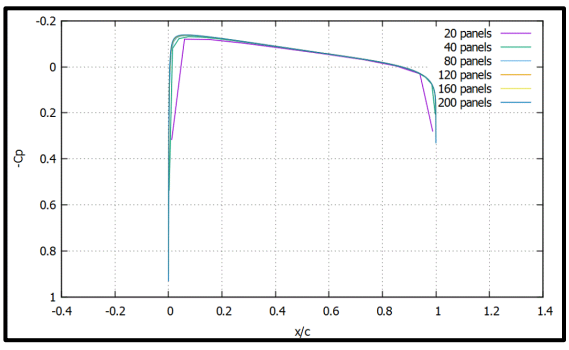

Fig. 2. Effect of Number of Panels on C_P Distribution for NACA0004 at AOA=zero.

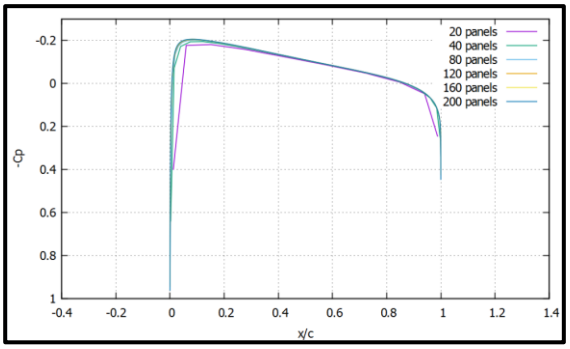

Fig. 3. Effect of Number of Panels on C_P Distribution for NACA0006 at AOA=zero.

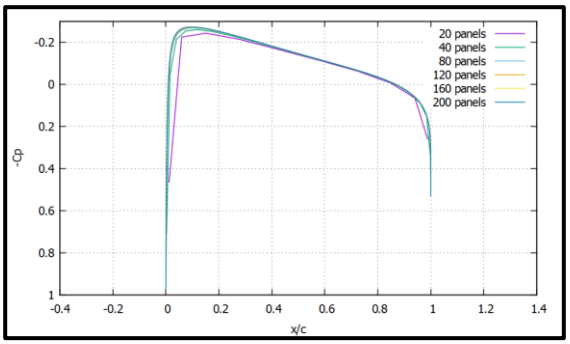

Fig. 4. Effect of Number of Panels on C_P Distribution for NACA0008 at AOA=zero.

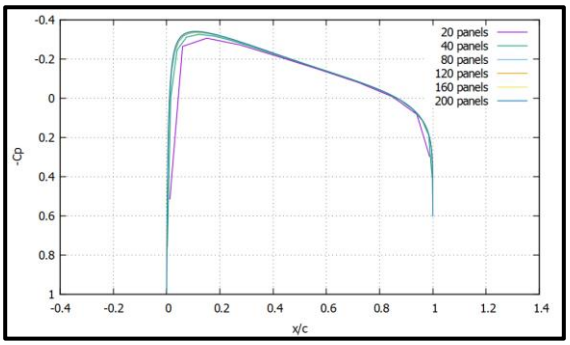

Fig. 5. Effect of Number of Panels on C_P Distribution for NACA0010 at AOA=zero.

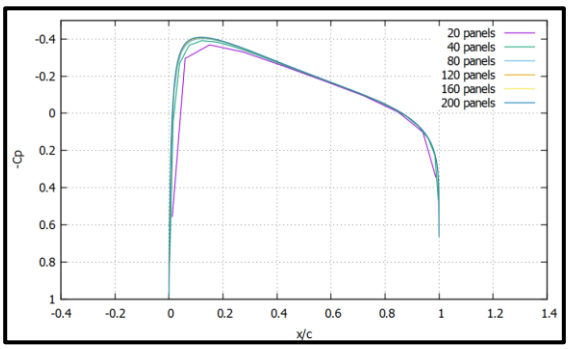

Fig. 6. Effect of Number of Panels on C_P Distribution for NACA0012 at AOA=zero.

The effect of the flow angle of attack on the panel count can be studied by examination of Figs. 7 to 10 a similar observation is made here: Both the solutions obtained by using twenty and forty panels have considerable deviations from the other obtained solutions in the vicinity of the leading as well as the trailing edge. Starting from eighty panels and increasing the panel count to two hundred has not led to any noticeable increase in the accuracy of the obtained solution.

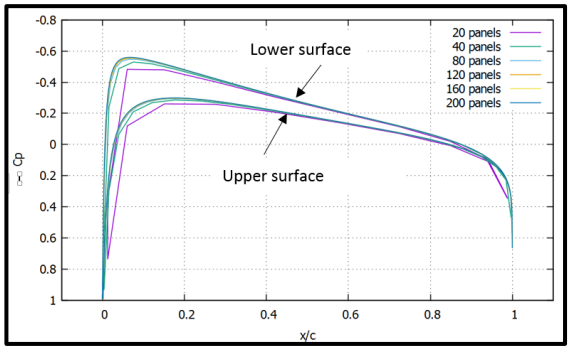

Fig. 7. Effect of Number of Panels on C_P Distribution at AOA=1° for NACA 0012.

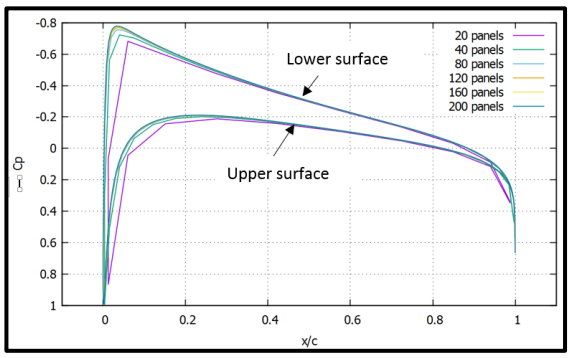

Fig. 8. Effect of Number of Panels on C_P Distribution at AOA=2° for NACA 0012.

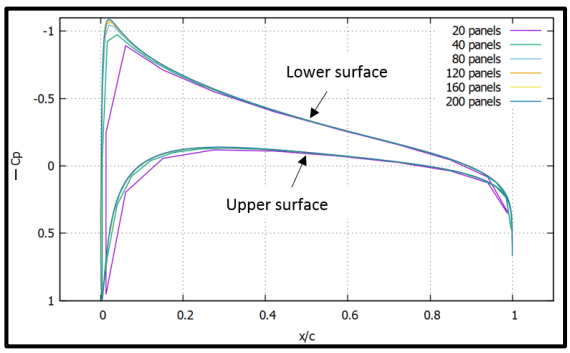

Fig. 9. Effect of Number of Panels on C_P Distribution at AOA =3° for NACA 0012.

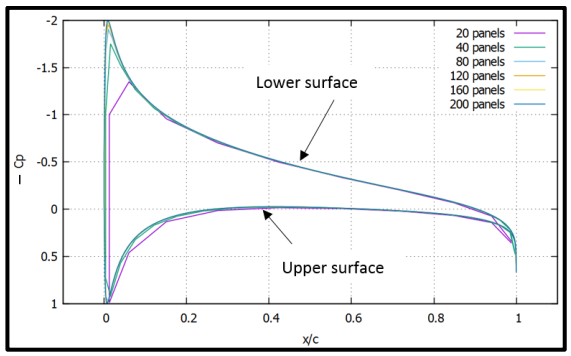

Fig. 10. Effect of Number of Panels on C_P Distribution at AOA=5° for NACA 0012.

3.2 Comparison of the Vortex Panel Method with the CFX

When it comes to choosing the test case, a special care must be taken. In other words, the test case must be chosen such that it lies within the field of application of the vortex panel method. It is well documented in the literature that vortex panel method is developed from the vortex sheet method, that is; it is originally formulated for a sheet or flat plate, and hence it can be extended to airfoils as long as the airfoils are thin.

Another aspect which should be considered when employing the vortex panel method is that it ignores the induced normal velocities on the surface of the airfoil and they are set equal to zero during the solution. This assumption is valid as long as the angle of attack is less than six degree; see (White, 2003). Accordingly, the test cases were chosen to be the flow around the NACA0012 at angles of attack of zero, one, two, three, four, five, and six degrees. Figs. 11 to 17 show the distribution of the coefficient of pressure versus the relative distance measured from the leading edge as obtained by the vortex panel method and by the CFX commercial program.

It should be noted here that the CFX was run based on input flow with a Mach number of 0.3 (incompressible flow) and selecting the laminar flow option. Examination of these six figures leads to two important observations: For angles of attack between zero and three degrees, the panel method solution is in good agreement with the CFX solution except at about 95% of the chord near the trailing edge. Slight deviations for ($0 < \propto < 3$) near the leading edge are also noticed that are related to the presence of the strong gradients near the stagnation point. The solution scheme of the CFX is strongly dependent on the values of these gradients. In contrast, the panel method does not depend on them.

The difference between the two solutions at the trailing edge is explained by the fact that the panel method employs the Kutta condition at the trailing edge whereas the CFX solves the laminar viscous flow past the airfoil. The second observation is that as the angle of attack is increased above three degrees, the solution of the panel method starts slightly to deviate (overestimate) the pressure on the higher-pressure side of the airfoil. This deviation occurs in the vicinity of the leading edge where the flow accelerates very fast from the stagnation point. In doing, so the flow will also pass the point at which the airfoil has the maximum thickness. Here it should be recalled that the panel method has the constraint of being limited to thin air foils and that the NACA0012 is a relatively thick airfoil. Increasing the angle of attack above three degrees will have an effect equivalent to increasing the airfoil thickness, see Fig. 18.

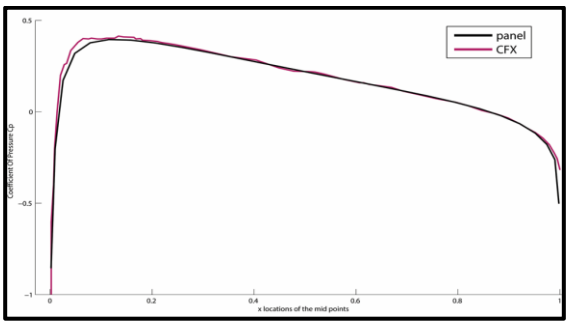

Fig. 11. C_P Distribution versus Distance from the Leading Edge for an AOA=zero.

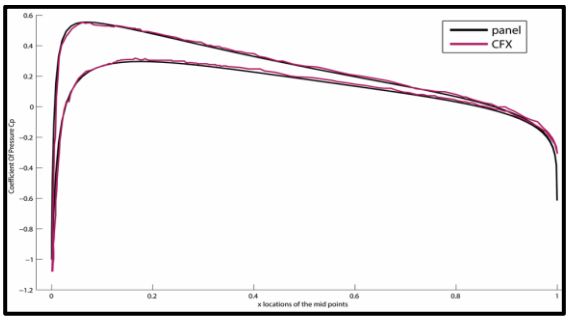

Fig. 12. C_P Distribution versus Distance from the Leading Edge for an AOA=1°.

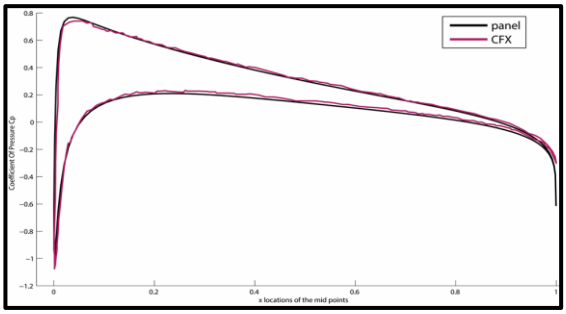

Fig. 13. C_P Distribution versus Distance from the Leading Edge for an AOA=2°.

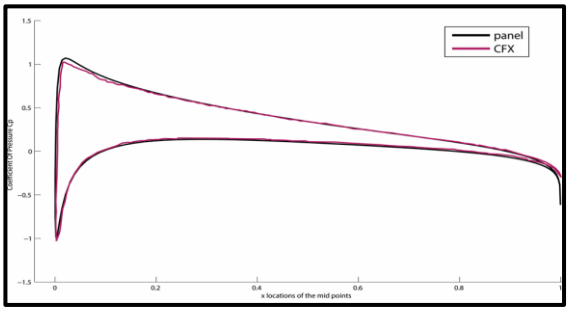

Fig. 14. C_P Distribution versus Distance from the Leading Edge for an AOA=3°.

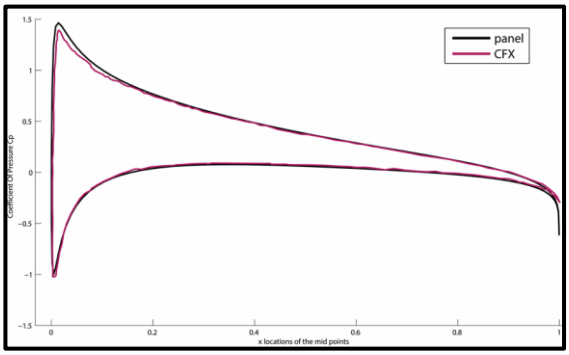

Fig. 15. C_P Distribution versus Distance from the Leading Edge for an AOA=4°.

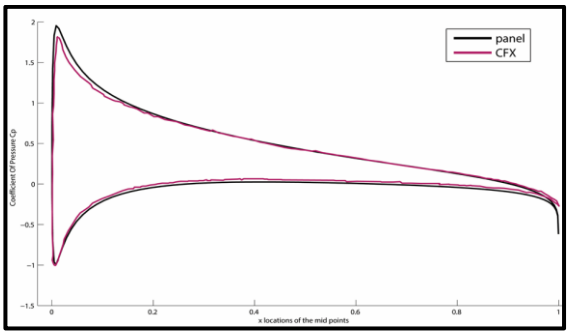

Fig. 16. C_P Distribution versus Distance from the Leading Edge for an AOA=5°.

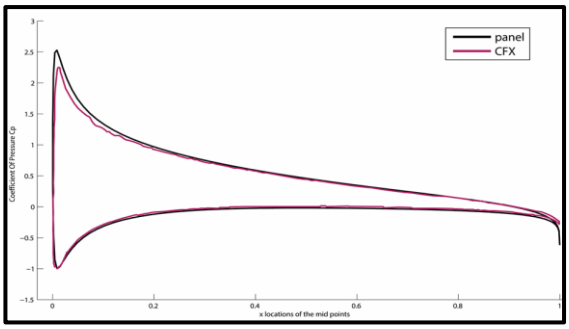

Fig. 17. C_P Distribution versus Distance from the Leading Edge for an AOA=6°.

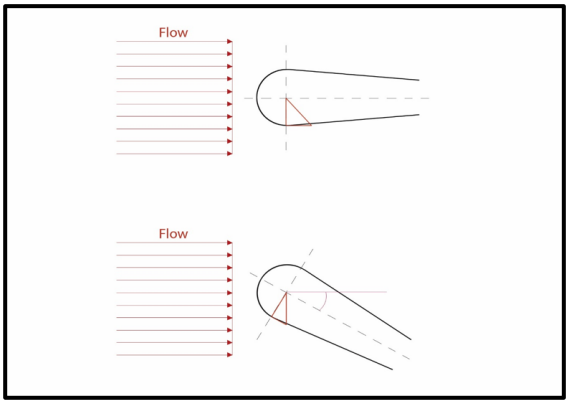

Fig. 18. Airfoil Thickness Change on the Lower Side due to the Increase in AOA.

3.3 Comparison of Panel Method Results with Results from Publications

In order to beef up the assessment process for the performance of the panel method, it was decided to compare its results with results published in the literature for the same test case. This has put a constraint on the selection of the test case. In other words, the authors of this paper were obliged to stick to that special test case which was selected by the authors of that published work. Moreover, most of the recent publications solve the full Navier−Stokes equations taking into account both compressibility and viscous effects. Nevertheless, this is one of the main reasons for this study, that is; to compare the result obtained by the panel method with that obtained by another more advanced yet sophisticated and time-consuming scheme. (Sengupta *et al.*, 2013) presented two different solutions for the flow past NACA0012 airfoil: The first solution is obtained for a compressible flow with a Mach number of 0.6 and an angle of attack of −0.14 degrees. The second solution is obtained for a near –transonic flow with Mach number of 0.758 and an angle of attack of −0.14 degrees. It should be noted that these two solutions were obtained for turbulent flow with Reynolds number of 3×10^6.

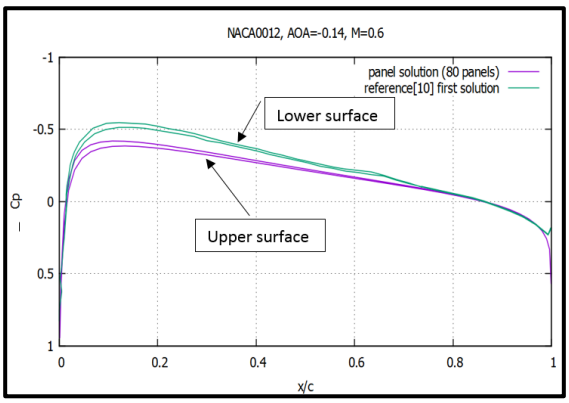

Fig. 19. Comparison of Panel Solution with the First Solution Given by (Sengupta *et al.*, 2013).

Fig. 19 shows a comparison of the first solution of (Sengupta *et al.*, 2013) with that obtained by the vortex panel method. It is very clear that the vortex panel method has performed well as compared to the numerically expensive other solution. Another comparison is shown in Fig. 20 where this time the second solution of (Sengupta *et al.*, 2013) is compared with that of the panel method.

Careful investigation of Fig. 20 delivers two important remarks: The first is that the vortex panel method solution deviates considerably from the solution of (Sengupta *et al.*, 2013). The second remark is that the vortex panel method solution has failed to capture the very weak shock waves that appear on both the lower and the upper surface of the airfoil. This behaviour of the vortex panel

method is pretty expected since this method was developed for incompressible flows that is; for flows with Mach number less than 0.3. As the Mach number is increased, the compressibility of the fluid is increased and accordingly the validity of the panel method will deteriorate. In the transonic flow range Mach number (0.8-1.2), weak shock waves will start to appear in the flow field. Shock waves are thin layers in the flow field through which steep gradients of the flow properties exist.

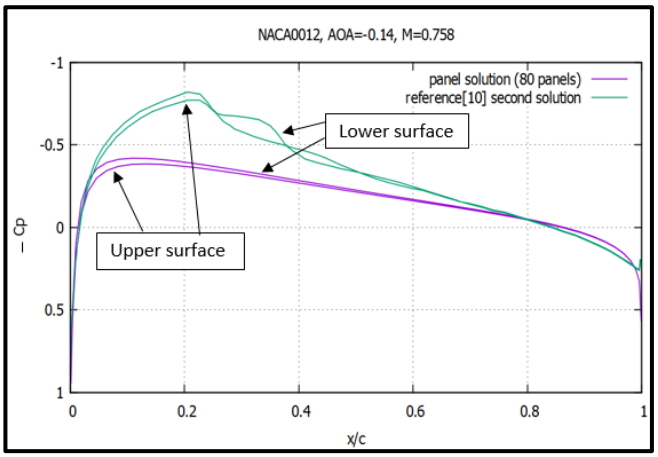

Fig. 20. Comparison of Panel Solution with Second Solution Given in (Sengupta *et al.*, 2013).

Special techniques* are usually incorporated in advanced flow solvers, like the one used by (Sengupta *et al.*, 2013) in order to enable the flow solver to detect the shock wave. Swanson and Lingers (2016) provide a solution for the flow past NACA0012 at Mach number of 0.5 and an angle of attack of zero. This solution was obtained by solving the complete Navier –Stokes equations for laminar flow at Reynolds number of 5000.

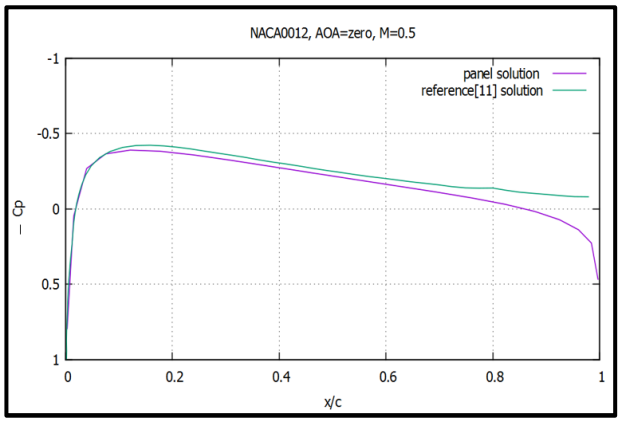

Fig. 21. Comparison of Panel Solution with Solution Given by (Swanson and Lingers, 2016).

Fig. 21 shows a comparison between the solution of the vortex panel method and the aforementioned solution from Swanson and Lingers (2016). As seen in this figure, the panel solution is in good agreement with the solution of Swanson and Lingers (2016) except at the trailing edge of the airfoil. This is again an expected behaviour from the panel method since it employs the Kutta condition (Eq. 8) in its derivation. At about 88% of the chord and before the trailing edge, (Swanson and Lingers, 2016) state that a flow separation will occur and a blow-up of streamline pattern can be clearly observed. Fig. 22 is taken from (Swanson and Lingers, 2016) and is presented here to clarify this phenomenon, which appears as a result of the viscous effect.

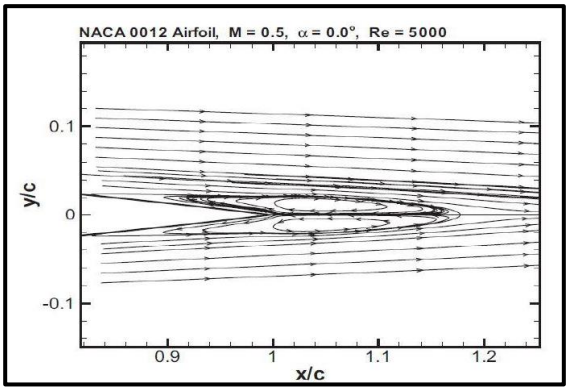

Fig. 22. Blow up of Streamline Pattern in the Airfoil Trailing Edge Region, from (Swanson and Lingers, 2016).

4. Conclusion

The vortex panel method is one of the first mathematical techniques that was used to solve the incompressible inviscid flow past thin airfoils. Since this method was developed originally for flat plate, the extension of its application to airfoils is limited to thin airfoils. The simplicity and compactness of the method have made it a very popular tool in hands of airplanes designers especially for making initial calculations at the early design stage. Another advantage of the vortex panel method is its low computational cost as compared to the computational cost of other more advanced compressible and viscous flow solvers. The results presented and discussed in this paper have shown that this method performs pretty well for thin airfoils and angle of attack of not more than four degrees provided that the flow is subsonic. If the flow is transonic, the vortex panel method was incapable of predicting and capturing even weak shock waves. One last conclusion that was drawn from the results is that the heavy dependence of the vortex panel method on the Kutta condition in its derivation has rendered it disable of capturing the flow separations and streamline's pattern blowups that appear at the trailing edge especially in turbulent flows.

This work can be further extended in a future study by studying the effect of camber and/or changing to another airfoil family, e.g. the NACA five or six-digits family.

Acknowledgments

The authors of this paper would like to thank Mr. Chris Kireney for his wonderful work on the vortex panel method, which is provided for public free of charge at: http://by.genie.uottawa.ca/~mcg4345/CompAssignments/vortexpanel-method.m

References

Anderson, J. D. (2010) Fundamentals of Aerodynamic, McGraw Hill Inc., Fifth Edition, 2010.

Josef Ballman, Richard Eppler, and Wolfgang Hackbush Hrsg. (1987) "Panel Method in Fluid Mechanics with Emphasis on Aerodynamics", Proceedings of Third GAMM Seminar-Kiel, January 16 to 18, 1987.

Chattot and Hafez, 2013) J. J. Chattot and M. M. Hafez "Theoretical and Applied Aerodynamics", Springer, Dordrecht, Heidelberg, and New York, 2013.

Daniel O. Dommasch, Sydney S. Sherby, and Thomas Connolly (1967) "Airplane Aerodynamics", Fourth Edition.

Gary A. Flandro, Howard M. McMahon, and Robert L. Roach (2012) "Basic Aerodynamic: Incompressible Flow", Cambridge University Press.

Katz J., and Plotkin A. (1991) "Low Speed Aerodynamics", McGraw Hill Inc. Series in Aeronautical and Aerospace Engineering, International Edition.

Kireny (2002) A Matlab Code by Chris Kireney Available Online at [http://by.genie.uottawa.ca/~mcg4345/CompAssignments/vortexpanelmethod.m].

Arnold M. Kuethe, and Chuen -Yen Chow (2009) "Foundations of Aerodynamics: Basic of Aerodynamic Design", Wiley India Inc., Fifth Edition.

Sengupta T. K., Bhole A., Sreejith N. A. (2013) 'Direct Numerical Simulation of 2D Transonic Flows around Airfoils', *Journal of Computers and Fluids*, 88, p.p. 19-37.

Swanson R.C., Lingers A. (2016) 'Steady -State Laminar Flow Solutions for NACA0012 Airfoil', *Journal of Computers and Fluids*, 126, p.p. 102-128.

Frank W. (2003) 'Fluid Mechanics'. McGraw Hill Series in Mechanical Engineering, Fifth Edition.

NOMENCLATURES

Latins:

A	Intermediate constant.
AOA	Angle of Attack.
$A_{n_{ij}}$	Influence coefficient for normal velocity.
$A_{t_{ij}}$	Influence coefficient for tangential velocity.
B	Intermediate constant.
C	Intermediate constant.
$C_{n1_{ij}}$, $C_{n2_{ij}}$	Coefficient for normal velocity.
$C_{t1_{ij}}$, $C_{t2_{ij}}$	Coefficient for tangential velocity.
C_p	Coefficient of pressure.
C_{p_i}	Pressure coefficient at control point.
D	Intermediate constant.
$\overrightarrow{d_s}$	Elemental vector.
E	Intermediate constant.
F	Intermediate constant.
G	Intermediate constant.
$\overrightarrow{n}$	Normal vector.
P	Intermediate constant.
Q	Intermediate constant.
Re	Reynolds number based on airfoil chord.
S_j	Length of the panel.
s_j	Distance measured from the leading edge.
t	Time.
$\overrightarrow{t}$	Tangential vector.
u	Velocity in x-coordinate.
$\vec{V}$	Vector velocity.
V_∞	Uniform velocity.
V_{n_i}	Normal velocity at control point.
V_{t_i}	Tangential velocity at control point.
V_i	Dimensionless velocity at control point.
v	Velocity in y-coordinate.
X_i	X-coordination at start point panel $\hat{\imath}^{th}$.
X_j	X-coordination at start point panel $\hat{\jmath}^{th}$.
x	X-coordinate.
x_i	X-coordination at mid-point panel $\hat{\imath}^{th}$.
Y_i	Y-coordination at start point panel $\hat{\imath}^{th}$.
Y_j	Y-coordination at start point panel $\hat{\jmath}^{th}$.
y	Y-coordinate.
y_i	Y-coordination at mid-point panel $\hat{\imath}^{th}$.
z	Z-coordinate.

Greeks:

θ_i	The orientation angle of the $\hat{\imath}^{th}$ panel.
θ_j	The orientation angle of the $\hat{\jmath}^{th}$ panel.
α	Angle of attack.
Γ	Circulation.
γ	Strength of the vortex
γ_j	Strength of the vortex at the start point
$\grave{\gamma}$	Dimensionless strength
ϕ	Velocity potential
ω	Velocity in z-coordinate
ρ	Density.
τ	Viscous stress.
ψ	Stream function.